

# The multiple electromagnetic wave scattering by small spheres

Justine Labat, Victor Péron, Sébastien Tordeux

PhD student in Mathematics

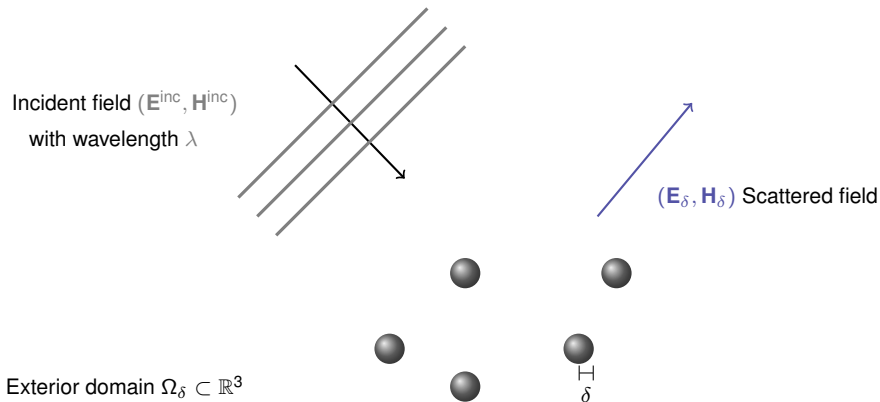
EPC Magique 3D — UPPA-E2S, INRIA Bordeaux Sud-Ouest, LMAP UMR CNRS 5142

Seminar of RTWH Aachen University

Aachen, December 4th 2018

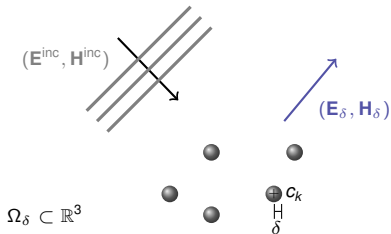


# 3D Scattering problem by small obstacles



Asymptotic assumption :  $\delta \ll \lambda$

# Model problem



- Time-harmonic domain
- Homogeneous & isotropic medium  $\Omega_\delta$
- Perfect conductors  $\mathcal{B}(c_k, \delta)$ ,  $k = 1 \dots N_{\text{obs}}$

## Time-harmonic Maxwell equations

$$\begin{cases} \mathbf{curl} \, \mathbf{E}_\delta - i\kappa \mathbf{H}_\delta = 0 & \text{in } \Omega_\delta \\ \mathbf{curl} \, \mathbf{H}_\delta + i\kappa \mathbf{E}_\delta = 0 & \text{in } \Omega_\delta \end{cases}$$

$$\text{with } \kappa^2 = \omega^2 \mu \left( \epsilon + \frac{i\sigma}{\omega} \right), \Im(\kappa) \geq 0$$

## Boundary condition

$$\mathbf{n} \times \mathbf{E}_\delta = -\mathbf{n} \times \mathbf{E}^{\text{inc}} \quad \text{on } \partial\Omega_\delta$$

## Silver-Müller radiation condition

$$r(\mathbf{H}_\delta \times \hat{\mathbf{x}} - \mathbf{E}_\delta) \xrightarrow[r \rightarrow \infty]{} 0 \quad \text{unif. in } \hat{\mathbf{x}} = \frac{\mathbf{x}}{r}$$

## Mathematical well-posedness

For any  $\mathbf{E}^{\text{inc}} \in \mathbf{H}_{\text{loc}}(\mathbf{curl}, \Omega_\delta)$  there exist a unique solution  $(\mathbf{E}_\delta, \mathbf{H}_\delta) \in \mathbf{H}_{\text{loc}}(\mathbf{curl}, \Omega_\delta)^2$  to the exterior Maxwell problem.

## Asymptotic models

- ✗ Restricted to small obstacles
- ✓ Low computational cost
- ✓ Meshless method

# Motivations

## Asymptotic models

- ✗ Restricted to small obstacles
- ✓ Low computational cost
- ✓ Meshless method

Multiple scattering



## Foldy-Lax model

- ✓ Interactions taken into account
- ✓ Low computational cost
- ✓ Meshless method

Superposition  
principle



## Born approximation

- ✗ No interaction between the obstacles
- ✓ Low computational cost
- ✓ Meshless method

# Motivations

## Asymptotic models

- ✗ Restricted to small obstacles
- ✓ Low computational cost
- ✓ Meshless method

Multiple scattering



## Foldy-Lax model

- ✓ Interactions taken into account
- ✓ Low computational cost
- ✓ Meshless method

Superposition  
principle



## Born approximation

- ✗ No interaction between the obstacles
- ✓ Low computational cost
- ✓ Meshless method

## High-order numerical solution

- ✗ High computational cost
  - ✗ volumical methods FEM, DG, ...
  - ~ boundary element methods
- ✗ Mesh refinement
- ✓ High-order spectral method

# Outline

## 1. Single electromagnetic scattering by small spheres

- Asymptotic models
- Numerical results
- Application: the Born approximation

## 2. Multiple electromagnetic scattering by small spheres

- Foldy-Lax model
- Spectral method
- Numerical results

## 3. Conclusions and perspectives

# Outline

## 1. Single electromagnetic scattering by small spheres

- Asymptotic models
- Numerical results
- Application: the Born approximation

## 2. Multiple electromagnetic scattering by small spheres

- Foldy-Lax model
- Spectral method
- Numerical results

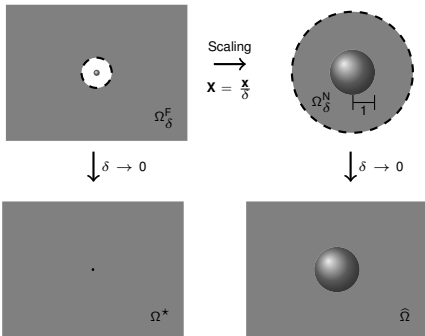
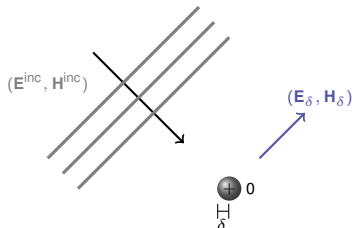
## 3. Conclusions and perspectives



# Approximation of solution to single scattering

## Method of **matched asymptotic expansions**

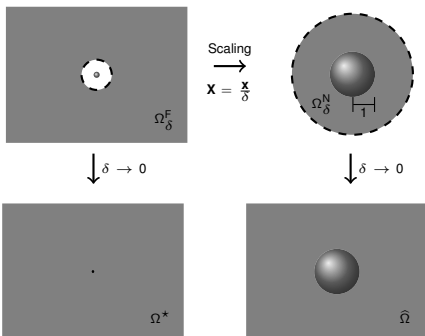
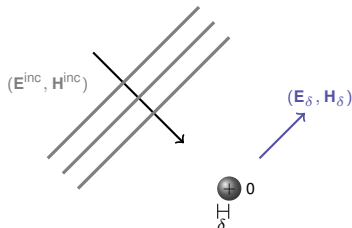
- Domain decomposition
- Local approximations
- Matching procedure



# Approximation of solution to single scattering

## Method of **matched asymptotic expansions**

- Domain decomposition
- **Local approximations**
- Matching procedure



## Asymptotic expansions

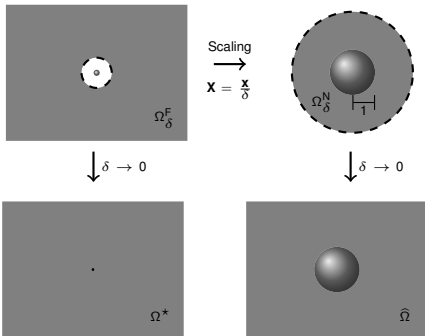
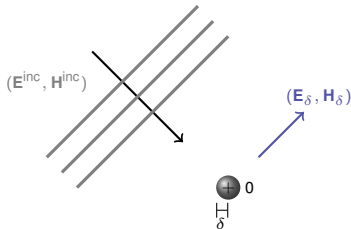
**Far field** expansion in  $\Omega^* = \mathbb{R}^3 \setminus \{0\}$

**Near field** expansion in  $\hat{\Omega} = \mathbb{R}^3 \setminus \overline{\mathcal{B}(0, 1)}$

# Approximation of solution to single scattering

## Method of **matched asymptotic expansions**

- Domain decomposition
- Local approximations
- **Matching procedure**



## Asymptotic expansions

**Far field** expansion in  $\Omega^* = \mathbb{R}^3 \setminus \{0\}$

**Near field** expansion in  $\hat{\Omega} = \mathbb{R}^3 \setminus \overline{\mathcal{B}(0, 1)}$

Near field



Far field

# Asymptotic expansions

## Near field expansion

$$\mathbf{E}_\delta(\delta\mathbf{X}) \approx \widehat{\mathbf{E}}_0(\mathbf{X}) + \delta\widehat{\mathbf{E}}_1(\mathbf{X}) + \delta^2\widehat{\mathbf{E}}_2(\mathbf{X}) + \dots$$

$$\mathbf{H}_\delta(\delta\mathbf{X}) \approx \widehat{\mathbf{H}}_0(\mathbf{X}) + \delta\widehat{\mathbf{H}}_1(\mathbf{X}) + \delta^2\widehat{\mathbf{H}}_2(\mathbf{X}) + \dots$$

$\mathbf{X} = \frac{\mathbf{x}}{\delta}$ : fast variable

## Far field expansion

$$\mathbf{E}_\delta(\mathbf{x}) \approx \delta^3\widetilde{\mathbf{E}}_3(\mathbf{x}) + \delta^4\widetilde{\mathbf{E}}_4(\mathbf{x}) + \delta^5\widetilde{\mathbf{E}}_5(\mathbf{x}) + \dots$$

$$\mathbf{H}_\delta(\mathbf{x}) \approx \delta^3\widetilde{\mathbf{H}}_3(\mathbf{x}) + \delta^4\widetilde{\mathbf{H}}_4(\mathbf{x}) + \delta^5\widetilde{\mathbf{H}}_5(\mathbf{x}) + \dots$$

- For an obstacle of arbitrary shape

Numerical solution of elementary problems **independent of  $\delta$**

- ▶ Near-field: **stationnary** problems
- ▶ Far-field: **time-harmonic** problems + equivalent multipole distributions

- For a **spherical** obstacle

- ▶ Analytical solutions of elementary problems
- ▶ Equivalent **multipole distributions**

# Equivalent multipole distributions

Boundary Value Problem



Problem in the free-space

$$\begin{cases} \operatorname{curl} \hat{\mathbf{E}}_0 = 0 & \text{in } \hat{\Omega} \\ \operatorname{div} \hat{\mathbf{E}}_0 = 0 & \text{in } \hat{\Omega} \\ \mathbf{n} \times \hat{\mathbf{E}}_0 = -\mathbf{n} \times \mathbf{E}^{\text{inc}}(0) & \text{on } \hat{\Gamma} \\ \hat{\mathbf{E}}_0 = O(R^{-1}) & R \rightarrow \infty \end{cases}$$

$$\hat{\mathbf{E}}_0 = -\nabla V_{1,\text{elec}}^{0,\text{stat}} = -\nabla \left( \lim_{\epsilon \rightarrow 0} V_{1,\text{elec}}^{\epsilon,\text{stat}} \right)$$

$$\begin{cases} -\Delta V_{1,\text{elec}}^{\epsilon,\text{stat}} = \varrho_1^\epsilon & \text{in } \mathbb{R}^3 \\ V_{1,\text{elec}}^{\epsilon,\text{stat}} = O(R^{-1}) & R \rightarrow \infty \end{cases}$$

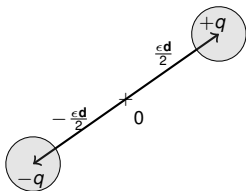


Figure: Electrostatic dipole

Distribution of two electric point-charges

$$\varrho_1^\epsilon = \frac{1}{\epsilon} \left( \delta_{\frac{\epsilon \mathbf{d}}{2}} - \delta_{-\frac{\epsilon \mathbf{d}}{2}} \right)$$

Dipole moment  $\mathbf{d}$  related to the BC

$$\mathbf{d} = 4\pi \mathbf{E}^{\text{inc}}(0)$$

# Equivalent multipole distributions

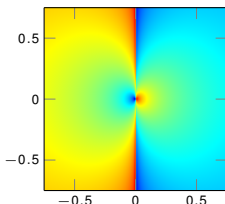
Boundary Value Problem



Problem in the free-space

$$\begin{cases} \mathbf{curl} \hat{\mathbf{E}}_0 = 0 & \text{in } \hat{\Omega} \\ \text{div} \hat{\mathbf{E}}_0 = 0 & \text{in } \hat{\Omega} \\ \mathbf{n} \times \hat{\mathbf{E}}_0 = -\mathbf{n} \times \mathbf{E}^{\text{inc}}(0) & \text{on } \hat{\Gamma} \\ \hat{\mathbf{E}}_0 = O(R^{-1}) & R \rightarrow \infty \end{cases}$$

$$\begin{cases} \text{div} \hat{\mathbf{E}}_0 = D\delta_0(\mathbf{d}) & \text{in } \mathbb{R}^3 \\ \mathbf{curl} \hat{\mathbf{E}}_0 = 0 & \text{in } \mathbb{R}^3 \end{cases}$$



Distribution of two electric point-charges

$$\varrho_1^\epsilon = \frac{1}{\epsilon} \left( \delta_{\frac{\epsilon \mathbf{d}}{2}} - \delta_{-\frac{\epsilon \mathbf{d}}{2}} \right)$$

Dipole moment  $\mathbf{d}$  related to the BC

$$\mathbf{d} = 4\pi \mathbf{E}^{\text{inc}}(0)$$

Figure: Electrostatic potential  $\epsilon \rightarrow 0$

# Equivalent multipole distributions

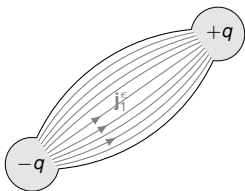
Boundary Value Problem



Problem in the free-space

$$\begin{cases} \operatorname{curl} \tilde{\mathbf{E}}_3 - i\kappa \tilde{\mathbf{H}}_3 = 0 & \text{in } \Omega^* \\ \operatorname{curl} \tilde{\mathbf{H}}_3 + i\kappa \tilde{\mathbf{E}}_3 = 0 & \text{in } \Omega^* \\ \tilde{\mathbf{E}}_3, \tilde{\mathbf{H}}_3 = O(r^{-3}) & r \rightarrow 0 \\ + \text{Silver-Müller condition} & \text{at } \infty \end{cases}$$

$$\begin{aligned} \tilde{\mathbf{E}}_3 &= -\nabla \left( \lim_{\epsilon \rightarrow 0} V_{1,\text{elec}}^\epsilon \right) + i\kappa \lim_{\epsilon \rightarrow 0} \mathbf{A}_{1,\text{elec}}^\epsilon \\ &\quad - \operatorname{curl} \lim_{\epsilon \rightarrow 0} \mathbf{A}_{1,\text{mag}}^\epsilon \\ \tilde{\mathbf{H}}_3 &= -\nabla \left( \lim_{\epsilon \rightarrow 0} V_{1,\text{mag}}^\epsilon \right) + i\kappa \lim_{\epsilon \rightarrow 0} \mathbf{A}_{1,\text{mag}}^\epsilon \\ &\quad + \operatorname{curl} \lim_{\epsilon \rightarrow 0} \mathbf{A}_{1,\text{elec}}^\epsilon \end{aligned}$$



Filiform current distribution

$$\mathbf{j}_1^\epsilon = \frac{i\omega}{\epsilon} \frac{\mathbf{d}_E}{|\mathbf{d}_E|} \delta_{\mathcal{F}_\epsilon}$$

Dipole moment  $\mathbf{d}_E$  related to  $\hat{\mathbf{E}}_0$

$$\mathbf{d}_E = 4\pi \mathbf{E}^{\text{inc}}(0)$$

Figure: Time-harmonic electric dipole

# Equivalent multipole distributions

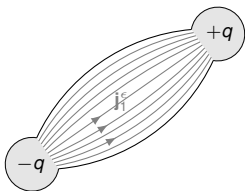
Boundary Value Problem



Problem in the free-space

$$\begin{cases} \mathbf{curl} \, \tilde{\mathbf{E}}_3 - i\kappa \tilde{\mathbf{H}}_3 = 0 & \text{in } \Omega^* \\ \mathbf{curl} \, \tilde{\mathbf{H}}_3 + i\kappa \tilde{\mathbf{E}}_3 = 0 & \text{in } \Omega^* \\ \tilde{\mathbf{E}}_3, \tilde{\mathbf{H}}_3 = O(r^{-3}) & r \rightarrow 0 \\ + \text{Silver-Müller condition} & \text{at } \infty \end{cases}$$

$$\begin{cases} -\Delta V_{1,\text{elec}}^\epsilon - \kappa^2 V_{1,\text{elec}}^\epsilon = \varrho_1^\epsilon & \text{in } \mathbb{R}^3 \\ + \text{Sommerfield condition} & R \rightarrow \infty \\ -\Delta \mathbf{A}_{1,\text{elec}}^\epsilon - \kappa^2 \mathbf{A}_{1,\text{elec}}^\epsilon = \frac{\mathbf{j}_1^\epsilon}{c} & \text{in } \mathbb{R}^3 \\ + \text{Sommerfield condition} & R \rightarrow \infty \end{cases}$$



Filiform current distribution

$$\mathbf{j}_1^\epsilon = \frac{i\omega}{\epsilon} \frac{\mathbf{d}_E}{|\mathbf{d}_E|} \delta_{\mathcal{F}_\epsilon}$$

Dipole moment  $\mathbf{d}_E$  related to  $\hat{\mathbf{E}}_0$

$$\mathbf{d}_E = 4\pi \mathbf{E}^{\text{inc}}(0)$$

Figure: Time-harmonic electric dipole



# Equivalent multipole distributions

Boundary Value Problem



Problem in the free-space

$$\begin{cases} \mathbf{curl} \, \tilde{\mathbf{E}}_3 - i\kappa \tilde{\mathbf{H}}_3 = 0 & \text{in } \Omega^* \\ \mathbf{curl} \, \tilde{\mathbf{H}}_3 + i\kappa \tilde{\mathbf{E}}_3 = 0 & \text{in } \Omega^* \\ \tilde{\mathbf{E}}_3, \tilde{\mathbf{H}}_3 = O(r^{-3}) & r \rightarrow 0 \\ + \text{Silver-Müller condition} & \text{at } \infty \end{cases}$$

$$\begin{cases} \mathbf{curl} \, \tilde{\mathbf{E}}_3 - i\kappa \tilde{\mathbf{H}}_3 = -i\kappa \mathbf{d}_H \delta_0 & \text{in } \mathbb{R}^3 \\ \mathbf{curl} \, \tilde{\mathbf{H}}_3 + i\kappa \tilde{\mathbf{E}}_3 = i\kappa \mathbf{d}_E \delta_0 & \text{in } \mathbb{R}^3 \\ \operatorname{div} \, \tilde{\mathbf{E}}_3 = D\delta_0(\mathbf{d}_E) & \text{in } \mathbb{R}^3 \\ \operatorname{div} \, \tilde{\mathbf{H}}_3 = D\delta_0(\mathbf{d}_H) & \text{in } \mathbb{R}^3 \\ + \text{Silver-Müller condition} & \text{at } \infty \end{cases}$$

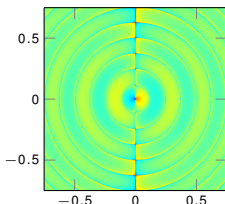


Figure: Electric potential  $\epsilon \rightarrow 0$

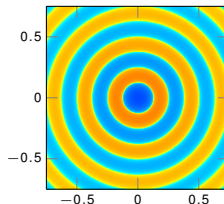


Figure: Magnetic potential  $\epsilon \rightarrow 0$

# Equivalent multipole distributions

$$\hat{\mathbf{E}}_p = \sum_{\substack{n=1 \\ |n-p| \text{ odd}}}^{p+1} \boldsymbol{\varepsilon}_{n,\text{elec}}^{\text{stat}}[\mathbf{u}_{1,n}^{p,E}, \dots, \mathbf{u}_{n,n}^{p,E}] + \sum_{\substack{n=1 \\ |n-p| \text{ even}}}^{p+1} \boldsymbol{\varepsilon}_{n,\text{mag}}^{\text{stat}}[\mathbf{u}_{1,n}^{p,H}, \dots, \mathbf{u}_{n,n}^{p,H}]$$

$$\tilde{\mathbf{E}}_{p+3} = \sum_{n=1}^{p+1} \left\{ \boldsymbol{\varepsilon}_{n,\text{elec}}[\mathbf{v}_{1,n}^{p,E}, \dots, \mathbf{v}_{n,n}^{p,E}] + \boldsymbol{\varepsilon}_{n,\text{mag}}[\mathbf{v}_{1,n}^{p,H}, \dots, \mathbf{v}_{n,n}^{p,H}] \right\}$$

	Order	Dipole		Quadrupole		Octupole	
		Electric	Magnetic	Electric	Magnetic	Electric	Magnetic
Near field	0	●	●				
	1						
	2						
Far field	3	● ●	● ●				
	4						
	5						

● Electric field

● Magnetic field

+ Far field **collected dipolar** model



J. Labat, V. Péron, S. Tordeux (Inria Research Report n°9169, Mars 2018)

Asymptotic Modeling of the Electromagnetic Scattering by Small Spheres Perfectly Conducting.

# Equivalent multipole distributions

$$\hat{\mathbf{E}}_p = \sum_{\substack{n=1 \\ |n-p| \text{ odd}}}^{p+1} \mathcal{E}_{n,\text{elec}}^{\text{stat}}[\mathbf{u}_{1,n}^{p,E}, \dots, \mathbf{u}_{n,n}^{p,E}] + \sum_{\substack{n=1 \\ |n-p| \text{ even}}}^{p+1} \mathcal{E}_{n,\text{mag}}^{\text{stat}}[\mathbf{u}_{1,n}^{p,H}, \dots, \mathbf{u}_{n,n}^{p,H}]$$

$$\tilde{\mathbf{E}}_{p+3} = \sum_{n=1}^{p+1} \left\{ \mathcal{E}_{n,\text{elec}}[\mathbf{v}_{1,n}^{p,E}, \dots, \mathbf{v}_{n,n}^{p,E}] + \mathcal{E}_{n,\text{mag}}[\mathbf{v}_{1,n}^{p,H}, \dots, \mathbf{v}_{n,n}^{p,H}] \right\}$$

	Order	Dipole		Quadrupole		Octupole	
		Electric	Magnetic	Electric	Magnetic	Electric	Magnetic
Near field	0	●	●				
	1	●	●	●	●		
	2						
Far field	3	● ●	● ●				
	4	● ●	● ●	● ●	● ●		
	5						

● Electric field

● Magnetic field

+ Far field **collected dipolar** model



J. Labat, V. Péron, S. Tordeux (Inria Research Report n°9169, Mars 2018)

Asymptotic Modeling of the Electromagnetic Scattering by Small Spheres Perfectly Conducting.

# Equivalent multipole distributions

$$\hat{\mathbf{E}}_p = \sum_{\substack{n=1 \\ |n-p| \text{ odd}}}^{p+1} \mathcal{E}_{n,\text{elec}}^{\text{stat}}[\mathbf{u}_{1,n}^{p,E}, \dots, \mathbf{u}_{n,n}^{p,E}] + \sum_{\substack{n=1 \\ |n-p| \text{ even}}}^{p+1} \mathcal{E}_{n,\text{mag}}^{\text{stat}}[\mathbf{u}_{1,n}^{p,H}, \dots, \mathbf{u}_{n,n}^{p,H}]$$

$$\tilde{\mathbf{E}}_{p+3} = \sum_{n=1}^{p+1} \left\{ \mathcal{E}_{n,\text{elec}}[\mathbf{v}_{1,n}^{p,E}, \dots, \mathbf{v}_{n,n}^{p,E}] + \mathcal{E}_{n,\text{mag}}[\mathbf{v}_{1,n}^{p,H}, \dots, \mathbf{v}_{n,n}^{p,H}] \right\}$$

	Order	Dipole		Quadrupole		Octupole	
		Electric	Magnetic	Electric	Magnetic	Electric	Magnetic
Near field	0	●	●				
	1	●	●	●	●		
	2	●	●	●	●	●	●
Far field	3	● ●	● ●				
	4	● ●	● ●	● ●	● ●		
	5	● ●	● ●	● ●	● ●	● ●	● ●

● Electric field

● Magnetic field

+ Far field **collected dipolar** model



J. Labat, V. Péron, S. Tordeux (Inria Research Report n°9169, Mars 2018)

Asymptotic Modeling of the Electromagnetic Scattering by Small Spheres Perfectly Conducting.

# Numerical validation

Small parameter

$$\delta \in \left\{ \frac{1}{10^p}, p = 0.5 : 0.1 : 4 \right\}$$

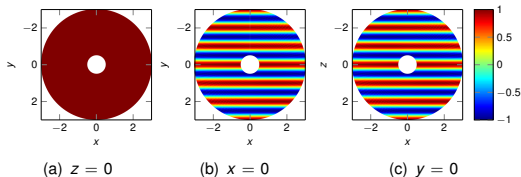


Figure: Incident plane wave (real part)

Physical parameters

- $\varepsilon = 1.0$
- $\mu = 1.0$
- $\sigma = 0$
- $\lambda = 5.0$

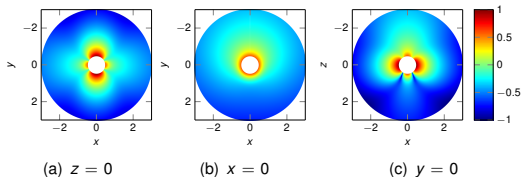


Figure: Reference scattered field (log)

# Numerical validation

Small parameter

$$\delta \in \left\{ \frac{1}{10^p}, p = 0.5 : 0.1 : 4 \right\}$$

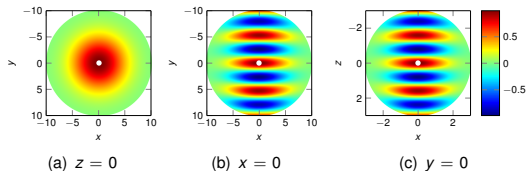


Figure: Incident **gaussian beam** (real part)

Physical parameters

- $\varepsilon = 1.0$
- $\mu = 1.0$
- $\sigma = 0$
- $\lambda = 5.0$

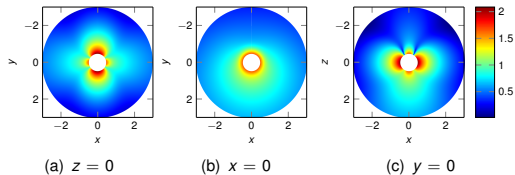


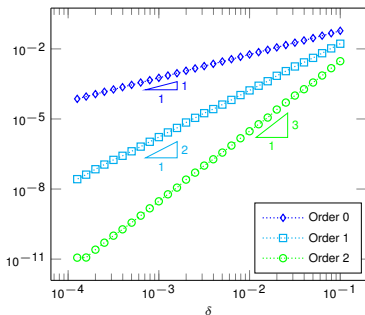
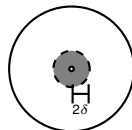
Figure: Reference scattered field (log)

# Numerical convergence of near field approximations

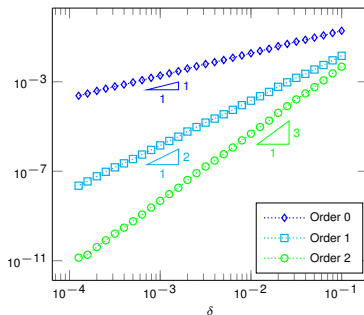
Order 0 :  $\|\mathbf{E}_\delta - \widehat{\mathbf{E}}_0(\frac{\cdot}{\delta})\|_{\mathbf{L}^2(\Omega_\delta^{2\delta})} / \|\mathbf{E}_\delta\|_{\mathbf{L}^2(\Omega_\delta^{2\delta})}$

Order 1 :  $\|\mathbf{E}_\delta - \widehat{\mathbf{E}}_0(\frac{\cdot}{\delta}) - \delta \widehat{\mathbf{E}}_1(\frac{\cdot}{\delta})\|_{\mathbf{L}^2(\Omega_\delta^{2\delta})} / \|\mathbf{E}_\delta\|_{\mathbf{L}^2(\Omega_\delta^{2\delta})}$

Order 2 :  $\|\mathbf{E}_\delta - \widehat{\mathbf{E}}_0(\frac{\cdot}{\delta}) - \delta \widehat{\mathbf{E}}_1(\frac{\cdot}{\delta}) - \delta^2 \widehat{\mathbf{E}}_2(\frac{\cdot}{\delta})\|_{\mathbf{L}^2(\Omega_\delta^{2\delta})} / \|\mathbf{E}_\delta\|_{\mathbf{L}^2(\Omega_\delta^{2\delta})}$



(a) Electric field



(b) Magnetic Field

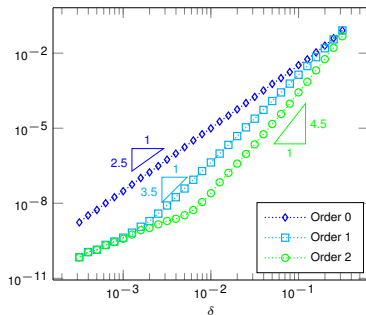
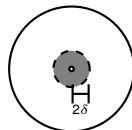
Figure: Relative  $\mathbf{L}^2(\Omega_\delta^{2\delta})$ -errors for near field approximations — Incident plane wave

# Numerical convergence of near field approximations

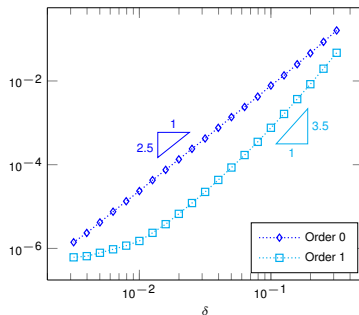
Order 0 :  $\|\mathbf{E}_\delta - \widehat{\mathbf{E}}_0(\frac{\cdot}{\delta})\|_{\mathbf{L}^2(\Omega_\delta^{2\delta})} / \|\mathbf{E}_\delta\|_{\mathbf{L}^2(\Omega_\delta^{2\delta})}$

Order 1 :  $\|\mathbf{E}_\delta - \widehat{\mathbf{E}}_0(\frac{\cdot}{\delta}) - \delta \widehat{\mathbf{E}}_1(\frac{\cdot}{\delta})\|_{\mathbf{L}^2(\Omega_\delta^{2\delta})} / \|\mathbf{E}_\delta\|_{\mathbf{L}^2(\Omega_\delta^{2\delta})}$

Order 2 :  $\|\mathbf{E}_\delta - \widehat{\mathbf{E}}_0(\frac{\cdot}{\delta}) - \delta \widehat{\mathbf{E}}_1(\frac{\cdot}{\delta}) - \delta^2 \widehat{\mathbf{E}}_2(\frac{\cdot}{\delta})\|_{\mathbf{L}^2(\Omega_\delta^{2\delta})} / \|\mathbf{E}_\delta\|_{\mathbf{L}^2(\Omega_\delta^{2\delta})}$



(a) Electric field



(b) Magnetic field

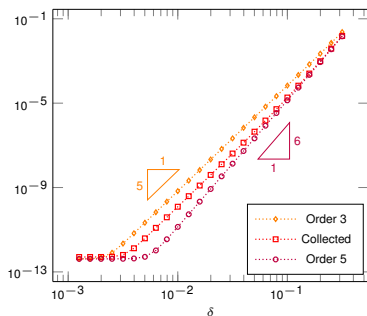
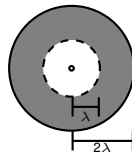
Figure: Relative  $\mathbf{L}^2(\Omega_\delta^{2\delta})$ -errors for near field approximations — Incident **gaussian beam**



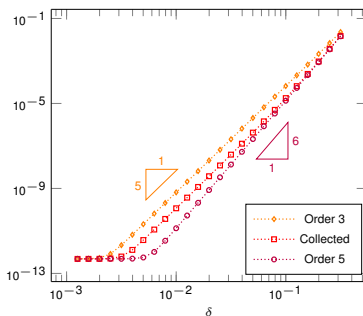
# Numerical convergence of far field approximations

Order 3 :  $\|\mathbf{E}_\delta - \delta^3 \tilde{\mathbf{E}}_3\|_{\mathbf{L}^2(\Omega_\lambda^{2\lambda})}$

Order 5 :  $\|\mathbf{E}_\delta - \delta^3 \tilde{\mathbf{E}}_3 - \delta^5 \tilde{\mathbf{E}}_5\|_{\mathbf{L}^2(\Omega_\lambda^{2\lambda})}$



(a) Electric field



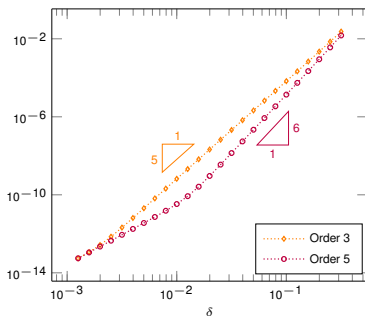
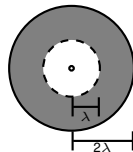
(b) Magnetic field

Figure: Absolute  $\mathbf{L}^2(\Omega_\lambda^{2\lambda})$ -errors for far field approximations — Incident plane wave

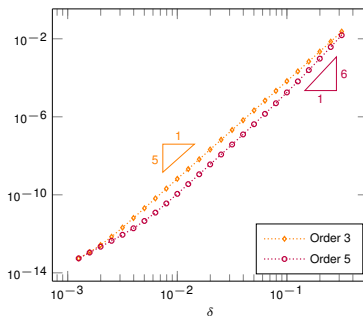
# Numerical convergence of far field approximations

Order 3 :  $\|\mathbf{E}_\delta - \delta^3 \tilde{\mathbf{E}}_3\|_{\mathbf{L}^2(\Omega_\lambda^{2\lambda})}$

Order 5 :  $\|\mathbf{E}_\delta - \delta^3 \tilde{\mathbf{E}}_3 - \delta^5 \tilde{\mathbf{E}}_5\|_{\mathbf{L}^2(\Omega_\lambda^{2\lambda})}$



(a) Electric field



(b) Magnetic field

Figure: Absolute  $\mathbf{L}^2(\Omega_\lambda^{2\lambda})$ -errors for far field approximations — Incident gaussian beam

## Application: the Born approximation

- The electric field is approximated by the **superposition principle**

$$\mathbf{E}_{\delta}(\mathbf{x}) \approx \sum_{k=1}^{N_{\text{obs}}} \mathbf{E}_{\delta,k}(\mathbf{x})$$

- Each obstacle is modeled as a **dipolar source** around  $c_k$

$$\mathbf{E}_{\delta,k}(\mathbf{x}) = \boldsymbol{\varepsilon}_{1,\text{elec}}[\mathbf{d}_{\delta,k}^{\text{E}}](\mathbf{x} - c_k) + \boldsymbol{\varepsilon}_{1,\text{mag}}[\mathbf{d}_{\delta,k}^{\text{H}}](\mathbf{x} - c_k)$$

- The dipole moments  $\mathbf{d}_{\delta,k}^{\text{E}}$  and  $\mathbf{d}_{\delta,k}^{\text{H}}$  depend on the nature of the obstacles

## Application: the Born approximation

- The electric field is approximated by the superposition principle

$$\mathbf{E}_{\delta}(\mathbf{x}) \approx \sum_{k=1}^{N_{\text{obs}}} \mathbf{E}_{\delta,k}(\mathbf{x})$$

- Each obstacle is modeled as a dipolar source around  $c_k$

$$\mathbf{E}_{\delta,k}(\mathbf{x}) = \mathcal{E}_{1,\text{elec}}[\mathbf{d}_{\delta,k}^{\text{E}}](\mathbf{x} - c_k) + \mathcal{E}_{1,\text{mag}}[\mathbf{d}_{\delta,k}^{\text{H}}](\mathbf{x} - c_k)$$

- The dipole moments  $\mathbf{d}_{\delta,k}^{\text{E}}$  and  $\mathbf{d}_{\delta,k}^{\text{H}}$  depend on the nature of the obstacles

For **perfectly conducting** spheres:

- Approximation of order 3

$$\mathbf{d}_{\delta,k}^{\text{E}} = 4\pi\delta^3 \mathbf{E}^{\text{inc}}(c_k)$$

$$\mathbf{d}_{\delta,k}^{\text{H}} = -2\pi\delta^3 \mathbf{H}^{\text{inc}}(c_k)$$

- Collected dipolar approximation

$$\mathbf{d}_{\delta,k}^{\text{E}} = 4\pi\delta^3 \left(1 + \frac{3(\kappa\delta)^2}{10}\right) \mathbf{E}^{\text{inc}}(c_k) \quad \mathbf{d}_{\delta,k}^{\text{H}} = -2\pi\delta^3 \left(1 - \frac{3(\kappa\delta)^2}{5}\right) \mathbf{H}^{\text{inc}}(c_k)$$

No interaction are taken into account

# Outline

## 1. Single electromagnetic scattering by small spheres

- Asymptotic models
- Numerical results
- Application: the Born approximation

## 2. Multiple electromagnetic scattering by small spheres

- Foldy-Lax model
- Spectral method
- Numerical results

## 3. Conclusions and perspectives

## Foldy-Lax model

- The electromagnetic fields are approximated by the superposition principle

$$\mathbf{E}_\delta(\mathbf{x}) \approx \sum_{k=1}^{N_{\text{obs}}} \mathbf{E}_{\delta,k}(\mathbf{x}) \quad \mathbf{H}_\delta(\mathbf{x}) \approx \sum_{k=1}^{N_{\text{obs}}} \mathbf{H}_{\delta,k}(\mathbf{x})$$

- Each obstacle is modeled as a dipolar source around  $c_k$

$$\begin{aligned} \mathbf{E}_{\delta,k}(\mathbf{x}) &= \mathcal{E}_{1,\text{elec}}[\mathbf{d}_{\delta,k}^{\text{E}}](\mathbf{x} - c_k) + \mathcal{E}_{1,\text{mag}}[\mathbf{d}_{\delta,k}^{\text{H}}](\mathbf{x} - c_k) \\ \mathbf{H}_{\delta,k}(\mathbf{x}) &= \mathcal{H}_{1,\text{elec}}[\mathbf{d}_{\delta,k}^{\text{E}}](\mathbf{x} - c_k) + \mathcal{H}_{1,\text{mag}}[\mathbf{d}_{\delta,k}^{\text{H}}](\mathbf{x} - c_k) \end{aligned}$$

For **perfectly conducting** spheres:

- Approximation of order 3

$$\mathbf{d}_{\delta,k}^{\text{E}} = 4\pi\delta^3 \left( \mathbf{E}^{\text{inc}}(c_k) + \sum_{\substack{\ell=1 \\ \ell \neq k}}^{N_{\text{obs}}} \mathbf{E}_{\delta,\ell}(c_k) \right) \quad \mathbf{d}_{\delta,k}^{\text{H}} = -2\pi\delta^3 \left( \mathbf{H}^{\text{inc}}(c_k) + \sum_{\substack{\ell=1 \\ \ell \neq k}}^{N_{\text{obs}}} \mathbf{H}_{\delta,\ell}(c_k) \right)$$

- Collected dipolar approximation

$$\mathbf{d}_{\delta,k}^{\text{E}} = 4\pi\delta^3 \left( 1 + \frac{3(\kappa\delta)^2}{10} \right) \left( \mathbf{E}^{\text{inc}}(c_k) + \sum_{\substack{\ell=1 \\ \ell \neq k}}^{N_{\text{obs}}} \mathbf{E}_{\delta,\ell}(c_k) \right) \quad \mathbf{d}_{\delta,k}^{\text{H}} = -2\pi\delta^3 \left( 1 - \frac{3(\kappa\delta)^2}{5} \right) \left( \mathbf{H}^{\text{inc}}(c_k) + \sum_{\substack{\ell=1 \\ \ell \neq k}}^{N_{\text{obs}}} \mathbf{H}_{\delta,\ell}(c_k) \right)$$

## Foldy-Lax model

- The electromagnetic fields are approximated by the superposition principle

$$\mathbf{E}_\delta(\mathbf{x}) \approx \sum_{k=1}^{N_{\text{obs}}} \mathbf{E}_{\delta,k}(\mathbf{x}) \quad \mathbf{H}_\delta(\mathbf{x}) \approx \sum_{k=1}^{N_{\text{obs}}} \mathbf{H}_{\delta,k}(\mathbf{x})$$

- Each obstacle is modeled as a dipolar source around  $c_k$

$$\begin{aligned}\mathbf{E}_{\delta,k}(\mathbf{x}) &= \boldsymbol{\varepsilon}_{1,\text{elec}}[\mathbf{d}_{\delta,k}^{\text{E}}](\mathbf{x} - \mathbf{c}_k) + \boldsymbol{\varepsilon}_{1,\text{mag}}[\mathbf{d}_{\delta,k}^{\text{H}}](\mathbf{x} - \mathbf{c}_k) \\ \mathbf{H}_{\delta,k}(\mathbf{x}) &= \boldsymbol{\mathcal{H}}_{1,\text{elec}}[\mathbf{d}_{\delta,k}^{\text{E}}](\mathbf{x} - \mathbf{c}_k) + \boldsymbol{\mathcal{H}}_{1,\text{mag}}[\mathbf{d}_{\delta,k}^{\text{H}}](\mathbf{x} - \mathbf{c}_k)\end{aligned}$$

- **Vectorial formulation** (3-order approximation)

Find  $\mathbf{d} = ((\mathbf{d}_1^E), \dots, (\mathbf{d}_{N_{\text{obs}}}^E), (\mathbf{d}_1^H), \dots, (\mathbf{d}_{N_{\text{obs}}}^H))^\top \in \mathbb{C}^{6N_{\text{obs}}}$  such that

$$\mathbf{d} - \delta^3 \mathbb{A} \mathbf{d} = \delta^3 \mathbf{f}$$

with  $\mathbf{f} = \begin{pmatrix} 4\pi \mathbf{E}^{\text{inc}}(c_1) \\ \vdots \\ 4\pi \mathbf{E}^{\text{inc}}(c_{N_{\text{obs}}}) \\ -2\pi \mathbf{H}^{\text{inc}}(c_1) \\ \vdots \\ -2\pi \mathbf{H}^{\text{inc}}(c_{N_{\text{obs}}}) \end{pmatrix}$  and  $\mathbb{A}$  the “interaction” matrix

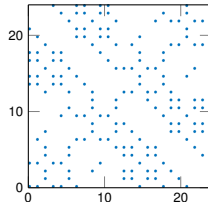


Figure: Skeleton of  $\mathbb{A}$  for  $N_{\text{obs}} = 4$

# Foldy-Lax approximations

- Approximation of order 3

$$\mathbf{d} - \delta^3 \mathbb{A} \mathbf{d} = \delta^3 \mathbf{f}$$

- Collected dipolar approximation

$$\mathbb{D}^{-1} \mathbf{d} - \delta^3 \mathbb{A} \mathbf{d} = \delta^3 \mathbf{f}$$

where

$$\mathbb{D} = \text{diag}(\underbrace{\alpha, \dots, \alpha}_{3N_{\text{obs}}}, \underbrace{\beta, \dots, \beta}_{3N_{\text{obs}}}) \quad \alpha = 1 + \frac{3(\kappa\delta)^2}{10} \quad \beta = 1 - \frac{6(\kappa\delta)^2}{10}$$

- Modified dipolar approximation

$$\tilde{\mathbb{D}}^{-1} \mathbf{d} - \delta^3 \mathbb{A} \mathbf{d} = \delta^3 \mathbf{f}$$

where

$$\tilde{\mathbb{D}} = \text{diag}(\underbrace{\tilde{\alpha}, \dots, \tilde{\alpha}}_{3N_{\text{obs}}}, \underbrace{\tilde{\beta}, \dots, \tilde{\beta}}_{3N_{\text{obs}}}) \quad \tilde{\alpha} = \frac{3i}{2(\kappa\delta)^3} \frac{j_1(\kappa\delta)}{h_1^{(1)}(\kappa\delta)} \quad \tilde{\beta} = -\frac{3i}{(\kappa\delta)^3} \frac{j_1(\kappa\delta) + \kappa\delta j_1'(\kappa\delta)}{h_1^{(1)}(\kappa\delta) + \kappa\delta h_1^{(1)'}(\kappa\delta)}$$



# Foldy-Lax approximations

- Approximation of order 3

$$\mathbf{d} - \delta^3 \mathbb{A} \mathbf{d} = \delta^3 \mathbf{f}$$

- Collected dipolar approximation

$$\mathbb{D}^{-1} \mathbf{d} - \delta^3 \mathbb{A} \mathbf{d} = \delta^3 \mathbf{f}$$

where

$$\mathbb{D} = \text{diag}(\underbrace{\alpha, \dots, \alpha}_{3N_{\text{obs}}}, \underbrace{\beta, \dots, \beta}_{3N_{\text{obs}}}) \quad \alpha = 1 + \frac{3(\kappa\delta)^2}{10} \quad \beta = 1 - \frac{6(\kappa\delta)^2}{10}$$

- **Modified** dipolar approximation

$$\tilde{\mathbb{D}}^{-1} \mathbf{d} - \delta^3 \mathbb{A} \mathbf{d} = \delta^3 \mathbf{f}$$

where

$$\tilde{\mathbb{D}} = \text{diag}(\underbrace{\tilde{\alpha}, \dots, \tilde{\alpha}}_{3N_{\text{obs}}}, \underbrace{\tilde{\beta}, \dots, \tilde{\beta}}_{3N_{\text{obs}}}) \quad \tilde{\alpha} = \frac{3i}{2(\kappa\delta)^3} \frac{j_1(\kappa\delta)}{h_1^{(1)}(\kappa\delta)} \quad \tilde{\beta} = -\frac{3i}{(\kappa\delta)^3} \frac{j_1(\kappa\delta) + \kappa\delta j_1'(\kappa\delta)}{h_1^{(1)}(\kappa\delta) + \kappa\delta h_1^{(1)'}(\kappa\delta)}$$

# Spectral method

- The electromagnetic fields are represented by the **Stratton-Chu formula** for  $\mathbf{x} \in \Omega_\delta$

$$\mathbf{E}_\delta(\mathbf{x}) = \sum_{k=1}^{N_{\text{obs}}} \mathbf{curl} \int_{\Gamma_\delta^k} \Phi(\mathbf{x}, \mathbf{y}) \mathbf{p}_k(\mathbf{y}) d\mathbf{S}_\mathbf{y}$$

where  $\Phi(\mathbf{x}, \mathbf{y}) = \frac{\exp(i\kappa|\mathbf{x}-\mathbf{y}|)}{4\pi|\mathbf{x}-\mathbf{y}|}$

# Spectral method

- The electromagnetic fields are represented by the Stratton-Chu formula for  $\mathbf{x} \in \Omega_\delta$

$$\mathbf{E}_\delta(\mathbf{x}) = \sum_{k=1}^{N_{\text{obs}}} \mathbf{curl} \int_{\Gamma_\delta^k} \Phi(\mathbf{x}, \mathbf{y}) \mathbf{p}_k(\mathbf{y}) d\mathbf{s}_y$$

- Each  $\mathbf{p}_k \in \mathbf{H}_t^{-\frac{1}{2}}(\text{div}_{\Gamma_\delta^k}, \Gamma_\delta^k)$  satisfies the **boundary integral equation**

$$\sum_{j=1}^{N_{\text{obs}}} \mathcal{M}_\Gamma^{kj} \mathbf{p}_j = -\mathbf{n} \times \mathbf{E}^{\text{inc}} \quad \text{on } \Gamma_\delta^k$$

where  $\mathcal{M}_\Gamma^{kj} : \mathbf{H}_t^{-\frac{1}{2}}(\text{div}_{\Gamma_\delta^j}, \Gamma_\delta^j) \longrightarrow \mathbf{H}_t^{-\frac{1}{2}}(\text{div}_{\Gamma_\delta^k}, \Gamma_\delta^k)$  is the extension of

$$\mathcal{M}_\Gamma^{kj} \lambda(\mathbf{x}_\Gamma) = \mathbf{n}(\mathbf{x}_\Gamma) \times \lim_{\mathbf{x} \rightarrow \mathbf{x}_\Gamma} \mathbf{curl} \int_{\Gamma_\delta^j} \Phi(\mathbf{x}, \mathbf{y}) \lambda(\mathbf{y}) d\mathbf{s}_y \quad \lambda \in \mathcal{C}^\infty(\Gamma_\delta^j) \quad \mathbf{x}_\Gamma \in \Gamma_\delta^k$$

# Spectral method

- The electromagnetic fields are represented by the Stratton-Chu formula for  $\mathbf{x} \in \Omega_\delta$

$$\mathbf{E}_\delta(\mathbf{x}) = \sum_{k=1}^{N_{\text{obs}}} \mathbf{curl} \int_{\Gamma_\delta^k} \Phi(\mathbf{x}, \mathbf{y}) \mathbf{p}_k(\mathbf{y}) d\mathbf{S}_\mathbf{y}$$

- Each  $\mathbf{p}_k \in \mathbf{H}_t^{-\frac{1}{2}}(\text{div}_{\Gamma_\delta^k}, \Gamma_\delta^k)$  satisfies the boundary integral equation

$$\sum_{j=1}^{N_{\text{obs}}} \mathcal{M}_\Gamma^{kj} \mathbf{p}_j = -\mathbf{n} \times \mathbf{E}^{\text{inc}} \quad \text{on } \Gamma_\delta^k$$

- Galerkin discretization of the BIE on local spectral basis with  $N_{\text{mod}}$  modes

$$\mathbf{p}_j(\mathbf{x}) = \sum_{n=1}^{N_{\text{mod}}} \sum_{m=-n}^n p_{n,m}^{j,\perp} \nabla_{\mathbb{S}^2} Y_{n,m}(\hat{\mathbf{x}}_j) + p_{n,m}^{j,\times} \mathbf{curl}_{\mathbb{S}^2} Y_{n,m}(\hat{\mathbf{x}}_j) \quad \mathbf{x} \in \Gamma_\delta^j$$

with  $\hat{\mathbf{x}}_j = \frac{\mathbf{x} - \mathbf{c}_j}{|\mathbf{x} - \mathbf{c}_j|}$  and  $\nabla_{\mathbb{S}^2} Y_{n,m}$ ,  $\mathbf{curl}_{\mathbb{S}^2} Y_{n,m}$ : complex-valued vector spherical harmonics

# Spectral method

- The electromagnetic fields are represented by the Stratton-Chu formula for  $\mathbf{x} \in \Omega_\delta$

$$\mathbf{E}_\delta(\mathbf{x}) = \sum_{k=1}^{N_{\text{obs}}} \mathbf{curl} \int_{\Gamma_\delta^k} \Phi(\mathbf{x}, \mathbf{y}) \mathbf{p}_k(\mathbf{y}) d\mathbf{S}_\mathbf{y}$$

- Each  $\mathbf{p}_k \in \mathbf{H}_t^{-\frac{1}{2}}(\text{div}_{\Gamma_\delta^k}, \Gamma_\delta^k)$  satisfies the boundary integral equation

$$\sum_{j=1}^{N_{\text{obs}}} \mathcal{M}_\Gamma^{kj} \mathbf{p}_j = -\mathbf{n} \times \mathbf{E}^{\text{inc}} \quad \text{on } \Gamma_\delta^k$$

- Galerkin discretization of the BIE on local spectral basis with  $N_{\text{mod}}$  modes

$$\mathbf{p}_j(\mathbf{x}) = \sum_{n=1}^{N_{\text{mod}}} \sum_{m=-n}^n p_{n,m}^{j,\perp} \nabla_{S^2} Y_{n,m}(\hat{\mathbf{x}}_j) + p_{n,m}^{j,\times} \mathbf{curl}_{S^2} Y_{n,m}(\hat{\mathbf{x}}_j) \quad \mathbf{x} \in \Gamma_\delta^j$$



M. Ganesh, S.C. Hawkins (2009)

A high-order algorithm for multiple electromagnetic scattering in three dimensions



H. Barucq, J. Chabassier, H. Pham, S. Tordeux (2017)

Numerical robustness of single-layer method with Fourier basis for multiple obstacle acoustic scattering in homogeneous media

# Vectorial formulation

- **Variational** formulation: Find  $\mathbf{p}_k \in \mathbf{H}_t^{-\frac{1}{2}}(\text{div}_{\Gamma_\delta^k}, \Gamma_\delta^k)$  such that

$$\langle \mathcal{M}_{\Gamma}^{kj} \mathbf{p}_j, \mathbf{v}_k \rangle_{\Gamma_\delta^k} = -\langle \mathbf{n} \times \mathbf{E}^{\text{inc}}, \mathbf{v}_k \rangle_{\Gamma_\delta^k} \quad \forall \mathbf{v}_k \in \mathbf{H}_t^{-\frac{1}{2}}(\text{curl}_{\Gamma_\delta^k}, \Gamma_\delta^k)$$

- **Vectorial** formulation: Find  $\mathbf{p} = ((p_{n,m}^{1,\perp}), \dots, (p_{n,m}^{N_{\text{obs}},\perp}), (p_{n,m}^{1,\times}), \dots, (p_{n,m}^{N_{\text{obs}},\times}))^\top \in \mathbb{C}^{\mathbf{N}}$  s.t.

$$\mathbf{M} \mathbf{p} = \mathbf{f}$$

with  $\mathbf{N} = 2N_{\text{mod}}(N_{\text{mod}} + 2)N_{\text{obs}}$  and

$$\mathbf{M} = \begin{pmatrix} \mathbf{M}_{\perp\perp} & \mathbf{M}_{\perp\times} \\ \mathbf{M}_{\times\perp} & \mathbf{M}_{\times\times} \end{pmatrix} \quad \text{with} \quad \mathbf{M}_{\alpha\beta} = \begin{pmatrix} \mathbf{M}_{\alpha\beta}^{11} & \mathbf{M}_{\alpha\beta}^{12} & \dots & \mathbf{M}_{\alpha\beta}^{1N_{\text{obs}}} \\ \mathbf{M}_{\alpha\beta}^{21} & \mathbf{M}_{\alpha\beta}^{22} & \dots & \mathbf{M}_{\alpha\beta}^{2N_{\text{obs}}} \\ \vdots & \vdots & \ddots & \vdots \\ \mathbf{M}_{\alpha\beta}^{N_{\text{obs}}1} & \mathbf{M}_{\alpha\beta}^{N_{\text{obs}}2} & \dots & \mathbf{M}_{\alpha\beta}^{N_{\text{obs}}N_{\text{obs}}} \end{pmatrix}$$

$$= \mathbf{M}_{\alpha\beta}(\delta, \mathbf{d}_{jk})$$



Y.-L. Xu (1995)

Electromagnetic scattering by an aggregate of small spheres

# Vectorial formulation

- Variational formulation: Find  $\mathbf{p}_k \in \mathbf{H}_t^{-\frac{1}{2}}(\text{div}_{\Gamma_\delta^k}, \Gamma_\delta^k)$  such that

$$\langle \mathcal{M}_{\Gamma}^{kj} \mathbf{p}_j, \mathbf{v}_k \rangle_{\Gamma_\delta^k} = -\langle \mathbf{n} \times \mathbf{E}^{\text{inc}}, \mathbf{v}_k \rangle_{\Gamma_\delta^k} \quad \forall \mathbf{v}_k \in \mathbf{H}_t^{-\frac{1}{2}}(\text{curl}_{\Gamma_\delta^k}, \Gamma_\delta^k)$$

- Vectorial formulation: Find  $\mathbf{p} = ((p_{n,m}^{1,\perp}), \dots, (p_{n,m}^{N_{\text{obs}},\perp}), (p_{n,m}^{1,\times}), \dots, (p_{n,m}^{N_{\text{obs}},\times}))^\top \in \mathbb{C}^N$  s.t.

$$\mathbb{M} \mathbf{p} = \mathbf{f}$$



Computation time  
Memory consumption  
Ill-conditioned system

- Anti-diagonal coefficients
- Number of unknowns
- Dense matrix



Mex interface (C)  
Preconditioning  
Smart storage and assembling

- Sub-blocks  $\mathbb{M}_{\alpha\beta}$  depend on  $\mathbf{d}_{jk}$
- Linear algebra
- Sparse matrix

# Linear transformations

$$\mathbf{E}_\delta = \phi_\delta(\mathbf{p}) \quad \text{with} \quad \mathbf{p} = \mathbf{p}(\delta, \mathbf{d}_{jk}) \quad \text{solves} \quad \mathbb{M} \mathbf{p} = \mathbf{f}$$

- **Step 1:** Change of variable  $\mathbb{T}_\delta$

$$\tilde{\mathbf{p}} := \mathbb{T}_\delta \mathbf{p} \quad \implies \quad \mathbf{E}_\delta = \phi(\tilde{\mathbf{p}})$$

- **Step 2:** Permutation matrix  $\mathbb{P}$

$$(\text{diag } \mathbb{P} \mathbb{M})_k \neq 0 \quad \forall k = 1, \dots, N$$

- **Step 3:** Diagonal matrix  $\mathbb{D}_\delta$

$$\tilde{\mathbb{M}} := \mathbb{D}_\delta^{-1} \mathbb{P} \mathbb{M} \quad \implies \quad (\text{diag } \tilde{\mathbb{M}})_k = 1 \quad \forall k = 1, \dots, N$$

$$\mathbf{E}_\delta = \phi(\tilde{\mathbf{p}}) \quad \text{with} \quad \tilde{\mathbf{p}} = \tilde{\mathbf{p}}(\delta, \mathbf{d}_{jk}) \quad \text{solves} \quad \tilde{\mathbb{M}} \tilde{\mathbf{p}} = \mathbb{D}_\delta^{-1} \mathbb{P} \mathbf{f}$$



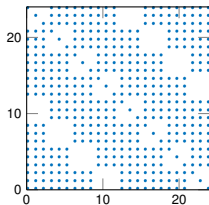
# Preconditionning

$$\mathbf{E}_\delta = \phi(\tilde{\mathbf{p}}) \quad \text{with} \quad \tilde{\mathbf{p}} = \tilde{\mathbf{p}}(\delta, \mathbf{d}_{jk}) \quad \text{solves} \quad \tilde{\mathbf{M}} \tilde{\mathbf{p}} = \mathbf{D}_\delta^{-1} \mathbf{P} \mathbf{f}$$

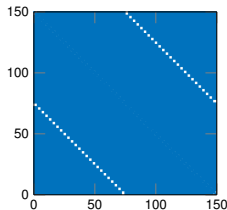


Number of unknowns  $\mathbf{N} = 2N_{\text{mod}}(N_{\text{mod}} + 2)N_{\text{obs}}$   
Dense matrix (approximation of coefficients)

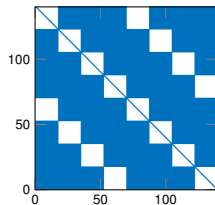
Memory consumption



(a)  $N_{\text{obs}} = 4$  and  $N_{\text{mod}} = 1$



(b)  $N_{\text{obs}} = 25$  and  $N_{\text{mod}} = 1$



(c)  $N_{\text{obs}} = 4$  and  $N_{\text{mod}} = 5$

Figure: Skeleton of  $\tilde{\mathbf{M}}$  ▶ Foldy

# Preconditionning

$$\mathbf{E}_\delta = \phi(\tilde{\mathbf{p}}) \quad \text{with} \quad \tilde{\mathbf{p}} = \tilde{\mathbf{p}}(\delta, \mathbf{d}_{jk}) \quad \text{solves} \quad \tilde{\mathbf{M}} \tilde{\mathbf{p}} = \mathbf{D}_\delta^{-1} \mathbf{P} \mathbf{f}$$

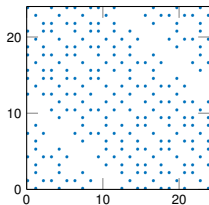


Number of unknowns  $\mathbf{N} = 2N_{\text{mod}}(N_{\text{mod}} + 2)N_{\text{obs}}$   
Dense matrix (approximation of coefficients)

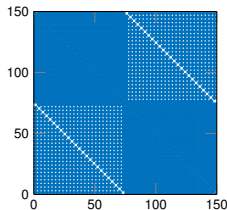
Memory consumption



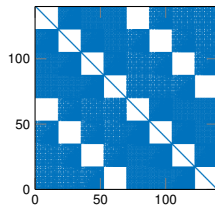
Error of approximation  
Analytic preconditionning (dipole)  
Algebraic preconditionning (small criterion)



(a)  $N_{\text{obs}} = 4$  and  $N_{\text{mod}} = 1$



(b)  $N_{\text{obs}} = 25$  and  $N_{\text{mod}} = 1$



(c)  $N_{\text{obs}} = 4$  and  $N_{\text{mod}} = 5$

Figure: Skeleton of  $\tilde{\mathbf{M}}$

# Preconditionning

$$\mathbf{E}_\delta = \phi(\tilde{\mathbf{p}}) \quad \text{with} \quad \tilde{\mathbf{p}} = \tilde{\mathbf{p}}(\delta, \mathbf{d}_{jk}) \quad \text{solves} \quad \tilde{\mathbf{M}} \tilde{\mathbf{p}} = \mathbf{D}_\delta^{-1} \mathbf{P} \mathbf{f}$$

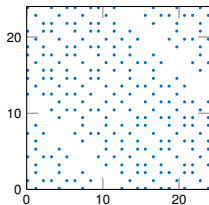


Number of unknowns  $\mathbf{N} = 2N_{\text{mod}}(N_{\text{mod}} + 2)N_{\text{obs}}$   
Dense matrix (approximation of coefficients)

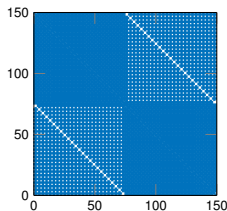
Memory consumption



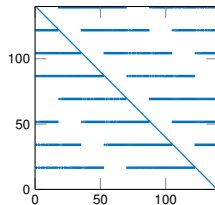
Error of approximation  
Analytic preconditionning (dipole)  
Algebraic preconditionning (small criterion)



(a)  $N_{\text{obs}} = 4$  and  $N_{\text{mod}} = 1$



(b)  $N_{\text{obs}} = 25$  and  $N_{\text{mod}} = 1$



(c)  $N_{\text{obs}} = 4$  and  $N_{\text{mod}} = 5$

Figure: Skeleton of  $\text{Precond}(\tilde{\mathbf{M}})$

# Preconditionning

$$\mathbf{E}_\delta = \phi(\tilde{\mathbf{p}}) \quad \text{with} \quad \tilde{\mathbf{p}} = \tilde{\mathbf{p}}(\delta, \mathbf{d}_{jk}) \quad \text{solves} \quad \tilde{\mathbf{M}} \tilde{\mathbf{p}} = \mathbf{D}_\delta^{-1} \mathbf{P} \mathbf{f}$$



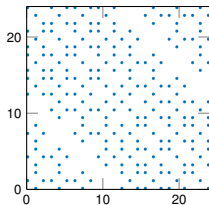
Number of unknowns  $\mathbf{N} = 2N_{\text{mod}}(N_{\text{mod}} + 2)N_{\text{obs}}$   
Dense matrix (approximation of coefficients)

Memory consumption

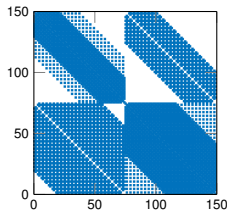


Error of approximation  
Analytic preconditionning (dipole)  
Algebraic preconditionning (small criterion)

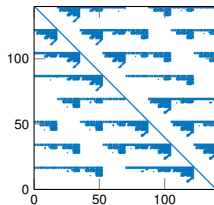
Sparse matrix



(a)  $N_{\text{obs}} = 4$  and  $N_{\text{mod}} = 1$



(b)  $N_{\text{obs}} = 25$  and  $N_{\text{mod}} = 1$



(c)  $N_{\text{obs}} = 4$  and  $N_{\text{mod}} = 5$

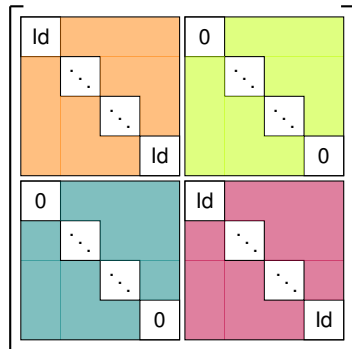
Figure: Skeleton of  $\text{Precond}(\tilde{\mathbf{M}})$

# Assembling for axisymmetric configurations

- Example: 4 aligned obstacles

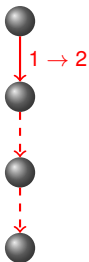


$$\tilde{\mathbf{M}} =$$



The sub-blocks  $\mathbf{M}_{\alpha\beta}^{kj}$  depend only on  $\delta$  and  $\mathbf{d}_{jk}$

- Example: 4 aligned obstacles



$$\tilde{\mathbf{M}} =$$

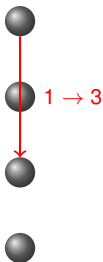
Figure 1 shows four 4x4 grids illustrating the construction of a 4x4 Latin square. The top row is labeled 'Id' and the bottom row is labeled '0'. The grids show the step-by-step filling of cells with numbers 1, 2, 3, and 4, using a diagonal pattern of dots to indicate the placement of the next number.

- Storage of sub-blocks



[illegible]



## Assembling for axisymmetric configurations

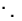

- Example: 4 aligned obstacles

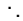
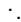


$$\tilde{\mathbf{M}} =$$

Id	1 - 2	1 - 3	
			
			
			Id

0			
			
			
			0

0			
			
			
			0

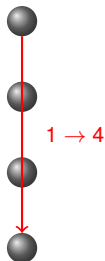
Id			
			
			
			Id

- Storage of sub-blocks

[illegible]

## Assembling for axisymmetric configurations

- Example: 4 aligned obstacles



$$\tilde{\mathbf{M}} =$$

Figure 1 shows four 4x4 grids illustrating the evolution of a 2D Ising spin system. Each grid contains a 4x4 lattice of spins (black dots) and their corresponding energy values (numbers) in the corners. The grids are labeled 'Id' (Identity) and '0' (Zero). The evolution shows the system moving from a high-energy state (Id) to a low-energy state (0) through a series of spin flips.

Id	1	2	3	4

0			

0			

Id			

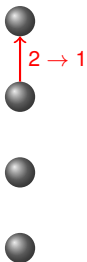
- Storage of sub-blocks

[illegible]



## Assembling for axisymmetric configurations

- Example: 4 aligned obstacles



$$\tilde{\mathbf{M}} =$$

Figure 1 displays four 4x4 grids illustrating the evolution of a 2D Ising spin system. Each grid shows a different stage of the system's state, with colors representing different spin configurations. The grids are labeled 'Id', '0', and '1' in the corners, indicating the system's state at that stage.

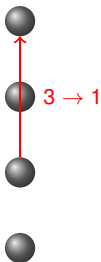
- Top Left Grid (labeled 'Id' in top-left):** Shows a state with a mix of colors (orange, yellow, green, blue, red). The top row is labeled '1 - 2 1 - 3 1 - 4'.
- Top Right Grid (labeled '0' in top-left):** Shows a state with a mix of colors (orange, yellow, green, blue, red). The top row is labeled '0'.
- Bottom Left Grid (labeled '0' in top-left):** Shows a state with a mix of colors (orange, yellow, green, blue, red). The top row is labeled '0'.
- Bottom Right Grid (labeled 'Id' in top-left):** Shows a state with a mix of colors (orange, yellow, green, blue, red). The top row is labeled 'Id'.

- Storage of sub-blocks

[illegible]

## Assembling for axisymmetric configurations

- Example: 4 aligned obstacles



$$\tilde{\mathbf{M}} =$$

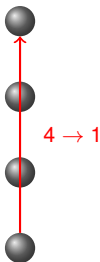
Figure 1 displays four 4x4 grids illustrating the evolution of a 2D Ising spin system. The grids are arranged in a 2x2 layout, showing the state of the system at different stages of evolution. The top-left grid shows the initial state with spins 1 (orange), -1 (pink), and 0 (white). The top-right grid shows the state after one iteration, with spins 0 (white), 1 (light green), and -1 (dark green). The bottom-left grid shows the state after two iterations, with spins 0 (white), 1 (light blue), and -1 (dark blue). The bottom-right grid shows the state after three iterations, with spins 0 (white), 1 (light purple), and -1 (dark purple). The evolution shows a transition from a disordered state to a more ordered state.

- Storage of sub-blocks

[illegible]

## Assembling for axisymmetric configurations

- Example: 4 aligned obstacles



$$\tilde{\mathbf{M}} =$$

Figure 1 displays four 4x4 grids illustrating the evolution of a 2D Ising spin system. The grids are labeled 0, 1, 2, and 3, representing the state of the system at different time steps.

- Grid 0:** The initial state. The diagonal cells (top-left to bottom-right) are black, while all other cells are white.
- Grid 1:** The state after one iteration. Black spins have spread to the cells immediately adjacent to the diagonal. The cells on the main diagonal and the cells immediately adjacent to it are black, while all other cells are white.
- Grid 2:** The state after two iterations. Black spins have spread further. The cells on the main diagonal, the cells immediately adjacent to it, and the cells immediately adjacent to those are black, while all other cells are white.
- Grid 3:** The state after three iterations. Black spins have spread even further. The cells on the main diagonal, the cells immediately adjacent to it, the cells immediately adjacent to those, and the cells immediately adjacent to those are black, while all other cells are white.

- Storage of sub-blocks

[illegible]

# Assembling for axisymmetric configurations

- Example: 4 aligned obstacles



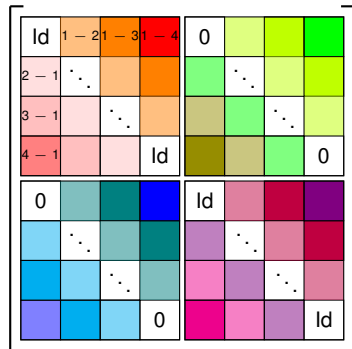
$8(N_{\text{obs}} - 1)$  blocks



instead of  $4(N_{\text{obs}})^2$



$$\tilde{\mathbf{M}} =$$



- Storage of sub-blocks



$N_{\text{obs}}$	$4(N_{\text{obs}})^2$	$8(N_{\text{obs}} - 1)$	Ratio (%)	$\tilde{\mathbf{M}}$ (GB)	$\tilde{\mathbf{M}}_{\text{Block}}$ (GB)
100	40 000	792	1.98	$5.76 \cdot 10^{-3}$	$1.15 \cdot 10^{-4}$
1 000	4 000 000	7 992	$1.998 \cdot 10^{-3}$	$5.76 \cdot 10^{-1}$	$1.15 \cdot 10^{-3}$
3 000	36 000 000	23 992	$6.664 \cdot 10^{-4}$	4.01	$3.45 \cdot 10^{-3}$
10 000	400 000 000	79 992	$1.9998 \cdot 10^{-4}$	--	$1.15 \cdot 10^{-2}$

## Assembling for axisymmetric configurations

- Example: 4 aligned obstacles

 $8(N_{\text{obs}} - 1)$  blocks

instead of  $4(N_{\text{obs}})^2$



$$\tilde{\mathbf{M}} =$$

Figure 1 displays four 4x4 grids illustrating the evolution of a 2D Ising spin system. The top-left grid shows the initial state with a diagonal of black spins and white spins elsewhere. The top-right grid shows the state after one iteration, with black spins spreading. The bottom-left grid shows the state after two iterations, with black spins forming a solid block. The bottom-right grid shows the state after three iterations, with black spins filling the entire grid.

- Storage of sub-blocks

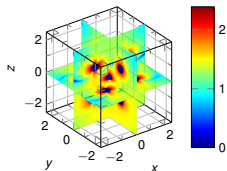
[illegible]

- Iterative solvers: define the **action** of  $\tilde{\mathbf{M}}_{\text{Block}}$  on  $\mathbf{u}$

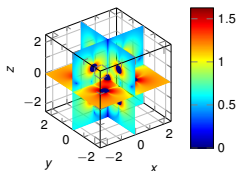
$$\mathcal{A}(\tilde{\mathbb{M}}_{\text{Block}}, \mathbf{u}) := \tilde{\mathbb{M}} \mathbf{u}$$

# Numerical validation

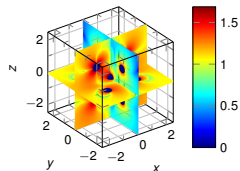
- 13 obstacles shared around the origin — **Arbitrary** configuration



(a) x-coordinates

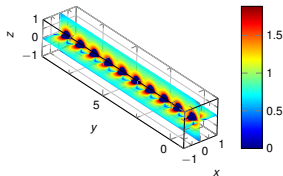


(b) y-coordinates

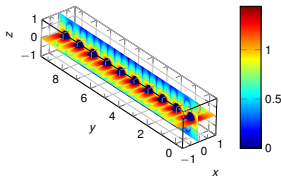


(c) z-coordinates

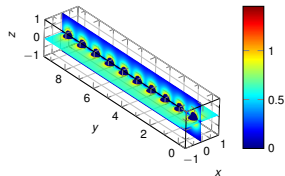
- 10 aligned obstacles — **Axisymmetric** configuration



(d) x-coordinates

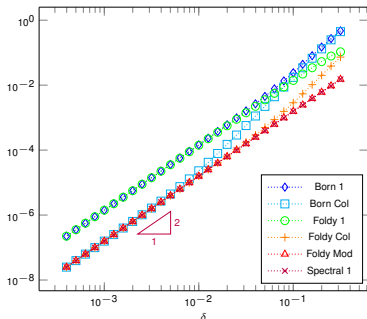


(e) y-coordinates

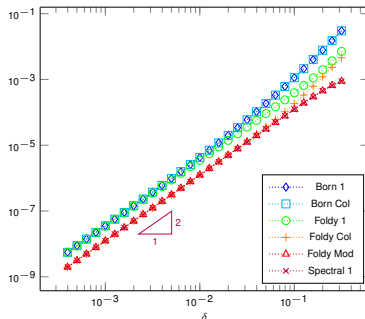


(f) z-coordinates

# Numerical convergence of reduced models



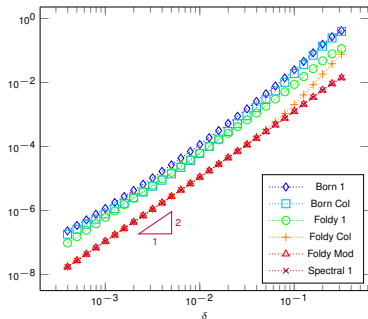
(g) Arbitrary configuration  $N_{\text{obs}} = 13$



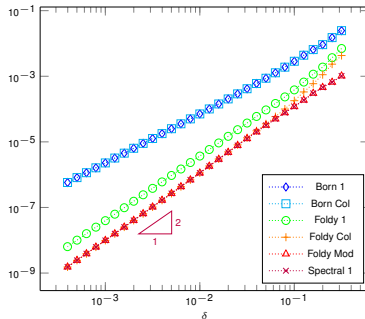
(h) Aligned obstacles  $N_{\text{obs}} = 20$

Figure: Relative  $L^2(\Omega_\lambda^{2\lambda})$ -errors for electric field with  $|\mathbf{d}_{jk}| \approx 1.0$

# Numerical convergence of reduced models



(a) Arbitrary configuration  $N_{\text{obs}} = 13$

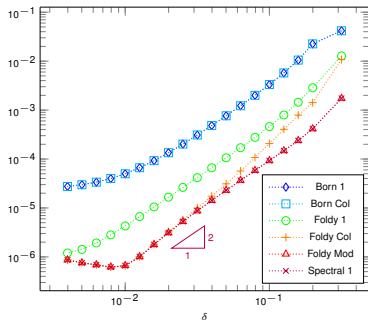


(b) Aligned obstacles  $N_{\text{obs}} = 20$

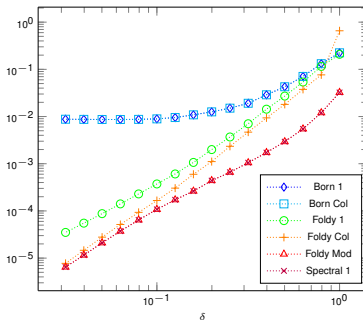
Figure: Relative  $\mathbf{L}^2(\Omega_\lambda^{2\lambda})$ -errors for electric field with  $|\mathbf{d}_{jk}| \approx 2\sqrt{\delta}$



# Numerical convergence of reduced models



(a) Arbitrary configuration  $N_{\text{obs}} = 13$



(b) Aligned obstacles  $N_{\text{obs}} = 20$

Figure: Relative  $L^2(\Omega_\lambda^{2\lambda})$ -errors for electric field with  $|\mathbf{d}_{jk}| \approx 4\delta$

# Time comparison

In terms of accuracy

Modified Foldy  $\longleftrightarrow$  Spectral 1

	Modified Foldy			Spectral 1 (arbitrary configuration)		
$N_{\text{obs}}$	100	1000	2000	100	1000	2000
Matrix	0.5588	51.0912	190.6899	10.0850	722.7368	5252
Right hand-side	0.000525	0.000648	0.0232	0.0045	0.0343	0.0722
Inversion	0.0157	7.1581	72.2991	0.0948	10.6212	90.1667
Time linear system	0.5750	58.2499	263.0122	10.1843	733.3923	5342.2
Representation	4.3079	48.4771	105.1629	4.2486	46.5048	89.4991
Total time	4.8829	106.7270	368.1751	14.4329	779.8971	5431.7

Table: Time computation in seconds

# Time comparison

In terms of accuracy

Modified Foldy  $\longleftrightarrow$  Spectral 1

	Modified Foldy			Spectral 1 (aligned configuration)		
$N_{\text{obs}}$	100	1000	2000	100	1000	2000
Matrix	0.5588	51.0912	190.6899	9.4903	105.2278	208.5052
Right hand-side	0.000525	0.000648	0.0232	0.0042	0.0320	0.0722
Inversion	0.0157	7.1581	72.2991	0.1656	10.8251	88.4188
Time linear system	0.5750	58.2499	263.0122	9.6001	116.0849	298.4607
Representation	4.3079	48.4771	105.1629	4.3087	44.6488	89.8913
Total time	4.8829	106.7270	368.1751	13.9088	160.7337	388.3520

Table: Time computation in seconds

# Outline

## 1. Single electromagnetic scattering by small spheres

- Asymptotic models
- Numerical results
- Application: the Born approximation

## 2. Multiple electromagnetic scattering by small spheres

- Foldy-Lax model
- Spectral method
- Numerical results

## 3. Conclusions and perspectives

# Conclusions and Perspectives

## Conclusion

- ✓ Numerical validation of the matched asymptotic expansions for single scattering
- ✓ Numerical validation of Born and Foldy-Lax models for multiple scattering
- ✓ Derivation and implementation of spectral method at any order

## On-going work

- ~ Smart assembling of spectral matrix for axisymmetric configurations
- ~ Numerical validation of spectral method with finite element solutions
- ~ Comparison of preconditionners and iterative solvers

## Perspectives

- ✗ Justification of the matched asymptotic expansions
- ✗ High-order Foldy-Lax models for multiple scattering
- ✗ Extension to time-dependent domain
- ✗ Numerical extension to obstacles of arbitrary shape

Thank you for your attention :)